LA-UR- 09-01539

Approved for public release;
distribution is unlimited.

Title:	Personal Dose Equivalent Conversion Coefficients for Neutron Fluence over the Energy Range of 20 to 250 MeV
Author(s):	Thomas D McLean, RP-2 Richard H. Olsher Allan L. Justus, RP-2 Robert T. Devine Milan S. Gadd, RP-2
Intended for:	Radiation Protection Dosimetry March 2009

Los Alamos
NATIONAL LABORATORY
EST. 1943

Los Alamos National Laboratory, an affirmative action/equal opportunity employer, is operated by the Los Alamos National Security, LLC for the National Nuclear Security Administration of the U.S. Department of Energy under contract DE-AC52-06NA25396. By acceptance of this article, the publisher recognizes that the U.S. Government retains a nonexclusive, royalty-free license to publish or reproduce the published form of this contribution, or to allow others to do so, for U.S. Government purposes. Los Alamos National Laboratory requests that the publisher identify this article as work performed under the auspices of the U.S. Department of Energy. Los Alamos National Laboratory strongly supports academic freedom and a researcher's right to publish; as an institution, however, the Laboratory does not endorse the viewpoint of a publication or guarantee its technical correctness.

Form 836 (7/06)

PERSONAL DOSE EQUIVALENT CONVERSION COEFFICIENTS FOR NEUTRON FLUENCE OVER THE ENERGY RANGE OF 20 TO 250 MEV

R. H. Olsher, T. D. McLean*, A.L. Justus, R.T. Devine and M.S. Gadd
Health Physics Measurements Group RP-2, MS J573, Los Alamos National Laboratory, Los Alamos, NM, 87545, USA

Monte Carlo simulations were performed to extend existing neutron personal dose equivalent fluence-to-dose conversion coefficients to an energy of 250 MeV. Presently, conversion coefficients, $H_{p,slab}(10,\alpha)/\Phi$, are given by ICRP-74 and ICRU-57 for a range of angles of radiation incidence (α =0, 15, 30, 45, 60, and 75 degrees) in the energy range from thermal to 20 MeV. Since neutron personal dose equivalent around high-energy accelerators is dominated by neutron leakage in the energy range of 10 to 200 MeV, neutron dosimetry at such facilities requires accurate conversion coefficients over this energy range. Previous calculations were based on the kerma approximation, which assumes that charged particle secondaries are locally deposited, or at least that charged particle equilibrium (CPE) exists within the tally cell volume. However, the kerma approximation is no longer valid in the energy range above 20 MeV and rigorous transport of secondary protons and other charged particle secondaries is a requirement for accurate absorbed dose calculations. The Los Alamos Monte Carlo radiation transport code MCNPX presently incorporates the necessary physics models to transport all secondary charged particles produced in neutron elastic and inelastic interactions. The recent addition of Heavy Ion (HI) physics has enabled the transport of heavy recoil nuclei such as carbon, nitrogen and oxygen in tissue. The MCNXP code was used to calculate all conversion functions and results are presented for a discrete set of angles of incidence on an ICRU tissue slab phantom.

INTRODUCTION

Presently, neutron conversion coefficients, $H_{p,slab}(10,\alpha)/\Phi$, are given by ICRP-74[1] and ICRU-57[2] for a range of angles of radiation incidence (α =0, 15, 30, 45, 60, and 75 degrees) in the energy range from thermal to 20 MeV. Since neutron personal dose equivalent around high-energy accelerators is dominated by neutron leakage in the energy range of 10 to 200 MeV, neutron dosimetry at such facilities requires accurate conversion coefficients over this energy range. Previous calculations[3-5] were based on the kerma approximation, which assumes that charged particle secondaries are locally deposited, or at least that charged particle equilibrium (CPE) exists within the tally cell volume. The kerma approximation was taken as a safe assumption for the energy range below 20 MeV, but it was recognized that it is no longer valid in the energy range above 20 MeV. In particular, the range of elastic recoil protons and protons produced during nonelastic nuclear interactions is significantly large in tissue (e.g., 4.5 cm at 75 MeV and 25 cm at 200 MeV). Thus, rigorous transport of secondary protons and other charged particle secondaries is a requirement for accurate absorbed dose calculations above 20 MeV.

The Los Alamos Monte Carlo radiation transport code MCNPX[6] was used to generate all of the conversion coefficients. Recent versions of this code incorporate the necessary physics models to transport all secondary charged particles produced in neutron elastic and inelastic interactions. Starting with version 26E[7], the Heavy Ion (HI) physics model has enabled the transport of recoil nuclei. Hence, heavy recoil nuclei (C, N and O) in tissue can now be transported in addition to the light ion types: proton, deuteron, triton, He-3, and alpha. The HI model automatically transports all residuals that are produced from any model physics (such as CEM[8], Bertini[9], etc.) interaction - even if the source particle is not a heavy ion. Neutron-produced carbon, nitrogen, and oxygen elastic recoils are transported (to a lower energy limit of 5 MeV) in the model regime if heavy ions are designated as live particles. Previously, it was only possible to transport light elastic recoils (proton, deuteron, He-3, and alpha) using the Light Ion Recoil model.

Transport within the cross section table regime does not normally create secondary particles, so any interaction using proton and neutron libraries typically will not produce transportable ions. The one significant exception is the LA150 cross section library[10] which provides neutron, proton, and photonuclear cross-sections up to 150 MeV (to 250 MeV for protons) for several ions (including H, C, N and O) based on experimental data and nuclear model calculations using the GNASH nuclear reaction model code. Above 20 MeV, secondary charge particle transport may be invoked for neutron interactions. Sampling is performed for proton, deuteron, triton, He-3

ion, and alpha production during each history. However, charged particle production is not correlated with neutron energy loss, but on average the correct number of charged particles are produced per nonelastic nuclear interaction.

Heating tallies in the model regime are based on collision physics. Local energy deposition can be determined for both light and heavy ions by specifying heating tallies for specific ion types. In order to obtain consistent collision-based heating tallies above a neutron energy of 20 MeV, the decision was made to use models instead of the LA150 cross section tables. The default Bertini INC[9] model was used for simulations up to a neutron energy of 200 MeV, while Cascade Exciton Model (CEM03.01)[10] physics were used for neutron and proton interactions above 200 MeV. CEM03.01 describes reactions induced by nucleons, pions, and photons as a three-stage process: Intranuclear Cascade (INC), followed by pre-equilibrium emission of particles during the de-excitation of the excited residual nuclei formed during the INC, followed by evaporation of particles from or fission of the compound nucleus. For both models, if the excited residual nucleus produced following the INC has a mass number, $A < 13$, a Fermi Breakup model is used to calculate its decay instead of considering a pre-equilibrium stage followed by evaporation from compound nuclei. The Bertini approach uses an older breakup model imported from the LAHET code[11], while CEM03.01 incorporates an updated and improved version of the LAHET breakup model, and also considers coalescence of complex particles up to ^{4}He from energetic nucleons emitted during the INC.

METHODS AND RESULTS

A parallel beam of neutrons was incident on 30 x 30 x 15 cm ICRU tissue slab phantom (10.1% H, 11.1% C, 2.6% N and 76.2% O by weight and of unit density). A rectangular area source of sufficient extent to fully irradiate the phantom was positioned 100 cm from the front face of phantom for the 0-degree irradiation geometry. A disc source was used for all other irradiation angles. Both the neutron beam and phantom were positioned in a void. The tally cell was defined as a thin rectangular volume, 4 cm x 4 cm x 0.1 cm, perpendicular to the beam axis and centered on the front face at a depth of 10mm. The intent was to approximate the dimensions of a personnel dosimeter located on the torso of a radiation worker and at the same time improve scoring efficiency.

Heating (F6) tallies in the model regime were specified for all live charged particles and heavy ions: F6:h, F16:d, F26:t, F36:s, F46:a, F56:e, and F96:# (the symbols following the colon are explained below). Charged particles were slowed down to a 1 keV cutoff energy, with the exception of heavy ions (1 MeV) and electrons and protons tracks outside of a spherical cell surrounding the tally volume (radius of 7 cm). Cutoffs outside of the sphere

were set 2 MeV for electrons and 25 MeV for protons as a variance reduction measure since tracks at or below these energies could not reach the tally cell.

The number of starting particle histories ranged from 1E08 to 1E09, depending on neutron energy, to give stochastic uncertainties on the order of 1%. Typical run times on a 3.8 GHz PC were on the order of 48 h at the highest energies per 1E09 histories.

The ICRP-60[12] Q(L) versus LET function was mapped as a function of energy using published ICRU-49[13] stopping powers for the charged particle secondaries (other than electrons). These functions, Q(E), were then convolved with the respective charged particle heating tallies during the slowing down process to obtain the sum, $\sum(\int D(L)Q(L)dL)$ in the tally cell for each particle type except electrons and heavy ions. The electron heating tally (F56:e) was added to the total to account for absorbed dose due to gamma tracks produced via inelastic interactions in the slab phantom. The heavy ion heating tally (F96:#) was multiplied by a quality factor of 20 to obtain the heavy ion dose equivalent.

Below 20 MeV, a conventional neutron track length heating tally was specified, which used cross section table kerma factors to calculate absorbed dose. Dose equivalent was obtained by folding tally F66:n with the mean Q for ICRU tissue[4]. Regardless of incident neutron energy, all heating tallies were converted from MeV/g to pGy and normalized per unit fluence. The $H_{p,slab}(10,\alpha)$ conversion factor per unit fluence for a given neutron energy and angle of incidence was then calculated as follows:

$$H_{p,slab}(10,\alpha)/\Phi = [(F6{:}h)Q_h(E) + (F16{:}d)Q_d(E) + (F26{:}t)Q_t(E) + (F36{:}s)Q_s(E) + (F46{:}a)Q_a(E) + (F56{:}e) + (F66{:}n)Q_m(E) + (F96{:}\#)(20)],$$

where $Q_h(E)$ is the quality factor function for protons,

$Q_d(E)$ is the quality factor function for deuterons,

$Q_t(E)$ is the quality factor function for tritons,

$Q_s(E)$ is the quality factor function for He-3 ions,

$Q_a(E)$ is the quality factor function for alpha particles,

$Q_m(E)$ is the mean quality factor for ICRU tissue[4]

To facilitate analysis of the data, Fortran routines were written to read, extract and organize the relevant tally data from the MCNPX output files and to calculate the Hp(10,α) dose conversion coefficient and its associated uncertainty.

In order to validate our computational model, it was applied to the calculation of ambient dose equivalent (using the ICRU sphere) at several neutron energies and the results were compared to published[1,2] conversion factors. Simulations were performed with both the Bertini and CEM.03 physics models to determine which model gave the better agreement. All simulations used a tally volume of 4 x 4 x 0.1 cm^3 at a depth of 10 mm in the ICRU sphere. The results are summarized in Table 1 where the overall uncertainty of these simulations is estimated as 10% (k=1) below 250 MeV. The Bertini INC model together with the LAHET Fermi Breakup model are seen to give the best overall agreement with published results in the range of 30 to 200 MeV.

Results for $H_{p,slab}(10, \alpha)/\Phi$ coefficients are given in Table 2. For comparison, ICRP-74[1]/ICRU-57[2] published values are also shown in parentheses at 10 and 20 MeV. The overall uncertainty of these simulations, including uncertainty inherent in the physics models, is estimated as 12% (k=1).

Fig.1 shows $H_{p,slab}(10, \alpha)/\Phi$ as a function of neutron energy at incident angles of 0, 45, 60 and 75 degrees (the 15 and 30 degree data were omitted for clarity as they were not readily distinguishable from the 0 degree points). At energies above 50 MeV, $H_{p,slab}(10,\alpha)/\Phi$ increases with angle of incidence where, on average, there is more material between incoming neutrons and the tally cell. Similar observations have been made by others[1,14,15] and has led to debate on the appropriateness of basing high-energy neutron dosimetry on the 10mm depth dose.

Fig. 2 gives the contribution of each particle type to the total personal dose equivalent as a function of energy for the 0-degree angle of incidence. The breakdown is similar for other angles of incidence. The major dose equivalent contribution is from alpha particle tracks, with heavy ions and proton tracks also being significant contributors. The neutron plot in this Figure refers to the sub-20 MeV heating tally. The sudden transition near 200 MeV in some of the particle plots (e.g. alpha) is due the mismatch between the Bertini and CEM models.

Fig. 3 shows a comparison of the current $H_{p,slab}(10,0)/\Phi$ calculation with ICRP-74(and ICRU-57) values of effective dose and ambient dose equivalent along with recent calculations of H*(10)[14,15]. Both $H_{p,slab}(10,0)$ and all H*(10) calculations are seen to underestimate E(AP) at neutron energies above 50 MeV. As has been pointed out in the literature[16-19], this is mainly a consequence of ICRP-60[10] recommendations overestimating the neutron weighting factor at energies above 100 MeV. The relatively slight differences between the current calculation of

$H_{p,slab}(10,0)$ and the H*(10) evaluations are reflective of the inherent uncertainties in the various physics models rather than differences in definition (*i.e.* slab vs spherical phantom).

CONCLUSION

Our results indicate that version 26E of the MCNPX code is capable of calculating $H_{p,slab}(10,\alpha)$, without recourse to the kerma approximation, by tracking all high-energy particle progeny generated during neutron interactions in tissue, in a rigourous yet straightforward manner. The present calculation of $H_{p,slab}(10,\alpha)/\Phi$ to 250 MeV is demonstration that the introduction of heavy ion transport in MCNPX will facilitate the calculation of any neutron dosimetric quantity at energies well above the kerma limit.

ACKNOWLEDGEMENT

REFERENCES

1. International Commission on Radiological Protection. *Conversion coefficients for use in radiological protection against external radiation.* ICRP Publication 74. Ann. ICRP 26(3/4) (Oxford: Pergamon Press) (1996).

2. International Commission on Radiological Units and Measurements. *Conversion coefficients for use in radiological protection against external radiation.* Report 57 (Bethesda, MD, USA: ICRU Publications) (1998).

3. Siebert, B.R.L. and Schuhmacher, H. *Calculated fluence-to-directional and personal dose equivalent conversion coefficients for neutrons.* Radiat. Prot. Dosim. **54**(3), 231-238 (1994).

4. Siebert, B.R.L. and Schuhmacher, H. *Quality factors, ambient and personal dose equivalent for neutrons, based on the new ICRU stopping powers for protons and alpha particles.* Radiat. Prot. Dosim. **58**(3),177-183 (1995).

5. Leuthold, G., Mares V. and Schraube, H., *On the Conservativity of Hp(10). Radiat. Prot. Dosim.* **70**(1-4), 379-382 (1997).

6. Waters, L.S.(ed.), *MCNPX, version 2.4.0.* Los Alamos National Laboratory report, LA-UR-02-5253 (August 2002).

7. Hendricks, J.S., McKinney, G.W., Fensin, M.L., James, M.R., Johns, R.C., Durkee, J.W., Finch, J.P., Pelowitz, D.B., Waters, L.S. and Gallmeier, F.X. *MCNPX, version 26E.* Los Alamos National Laboratory report, LA-UR-07-6632 (November 2007).

8. Mashnik, S.G., Sierk, A.J., Gudima K.K. and Baznat M.I. *CEM03 and LAQGSM03 – new modeling tools for nuclear applications.* J. Phys., Conf. Ser. **41**(1), 340-351 (2006).

9. Bertini, H.W., *Low-energy intranuclear cascade calculation.* Phys. Rev. **131**(4), 1801-1821 (1963).

10. Chadwick, M. B., Young, P. G., Chiba S., Frankle, S., Hale, G. M., Hughes, H. G., Koning, A. J., Little, R. C. MacFarlane, R. E., Prael, R. E., and Waters, L. S. *Cross section evaluations to 150 MeV for accelerator-driven systems and implementation in MCNPX.* Los Alamos National Laboratory Report LA-UR-98-1825 (1998).

11. Prael, R.E and Lichtenstein, H., *User guide to LSC: The LAHET code system.* Los Alamos National Laboratory report, LA-UR-89-3014 (1989).

12. International Commission on Radiological Protection. *1990 Recommendations of the International Commission on Radiological Protection.* ICRP Publication 60. Ann. ICRP 21(1/3) (Oxford: Pergamon Press) (1991).

13. International Commission on Radiation Units and Measurements. *Stopping powers and ranges for protons and alpha particles.* Report 57 (Bethesda, MD, USA: ICRU Publications) (1993).

14. Sannikov, A.V. and Savitskaya, E.N. *Ambient Dose Equivalent Conversion Factors for High Energy Neutrons based on ICRP 60 Recommendations.* Radiat. Prot. Dosim. 70, 383-386 (1997).

15. Pelliccioni, M. *Overview of the fluence-to-effective dose and fluence-to-ambient dose equivalent conversion coefficients for high energy radiation calculated using the Fluka code.* Radiat. Prot. Dosim. **88**(4), 279-297 (2000).

16. Leuthold, G. and Schraube, H. *Critical analysis of the ICRP-60 proposals for neutron radiation and a possible solution.* Radiat. Prot. Dosim. **54**, 217-220 (1994).

17. Yoshizawa, N., Sato, O., Takagi, S., Furihata, S., Iwai, S., Uehara, T., Tanaka, S., Sakamoto, Y. *External radiation conversion coefficients using radiation weighting factor and quality factor for neutron and proton from 20 MeV to 10 GeV.* J. Nucl. Sci. Technol. **35**(12), 928-942 (1998).

18. Ferrari, A. and Pelliccioni, M. *Fluence to dose equivalent conversion data and effective quality factors for high energy neutrons.* Radiat. Prot. Dosim. **76**(4), 215-224 (1998).

19. Thomas, R.H. *The impact of ICRP/ICRU quantities on high energy neutron dosimetry: a review.* Radiat. Prot. Dosim. **96**(4), 407-422 (2001)

Figure Captions

Fig. 1 $H_{p,slab}(10,\alpha)/\Phi$ for neutrons over the energy range of 20 to 250 MeV as a function of angle of incidence.

Fig. 2 Contribution of each particle type to the total personal dose equivalent conversion factor as a function of neutron energy for a 0-degree angle of incidence.

Fig. 3 A comparison of the current $H_{p,slab}(10,0)/\Phi$ calculation with previous effective dose and ambient dose equivalent calculations.

Table 1: H*(10)/Φ pSvcm^2		
Neutron Energy (MeV)	MCNPX	ICRP-74/ICRU-57 Table A.42
20	590	600
30	536 (Bertini)/461 (CEM)	515
50	395 (Bertini)/332 (CEM)	400
75	320 (Bertini)/261 (CEM)	330
100	288 (Bertini)/247 (CEM)	285
125	288 (Bertini)/258 (CEM)	260
150	281 (Bertini)/261 (CEM)	245
175	263 (Bertini)/245 (CEM)	250
201	262 (Bertini)/242 (CEM)	260

Table 2: $H_{pslab}(10,d)/\Phi$ MCNPX Simulation Results (pSv cm^2)						
E_n (MeV)	0-deg	15-deg	30-deg	45-deg	60-deg	75-deg
10	466 (480)	467 (481)	470 (497)	471 (493)	460 (480)	402 (421)
20	609 (600)	611 (595)	616 (619)	623 (615)	626 (619)	581 (570)
25	580	586	596	601	597	585
30	559	562	569	577	586	576
35	512	515	526	535	550	550
40	461	460	469	479	498	501
50	414	414	430	443	463	466
60	380	382	385	401	420	435
70	351	355	366	377	393	404
80	321	324	337	346	364	377
90	305	307	315	324	348	363
100	302	303	313	326	341	361
125	302	297	304	321	338	362
150	298	296	304	322	340	364
175	273	277	281	297	316	337
200	272	275	282	298	315	331
225	258	255	266	278	294	316
250	263	258	268	278	291	310

Figure 1

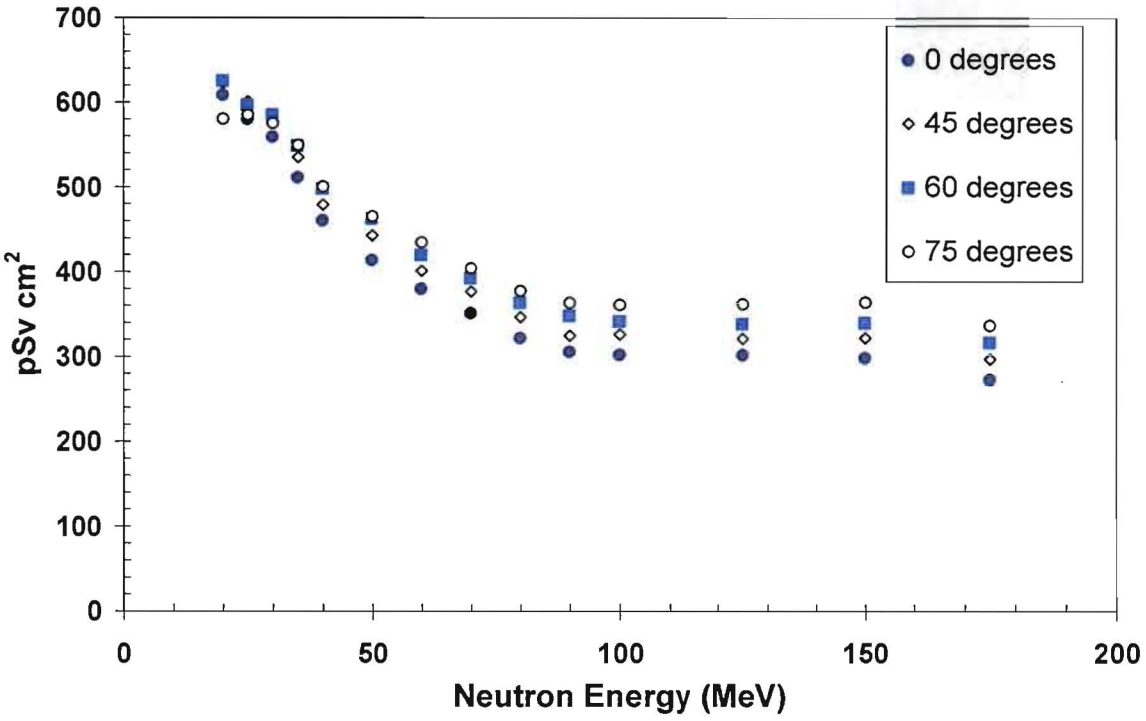
700
600
500
400
300
200
100
0
pSv cm2
0
50
100
150
200
Neutron Energy (MeV)
0 degrees
45 degrees
60 degrees
75 degrees

Figure 2

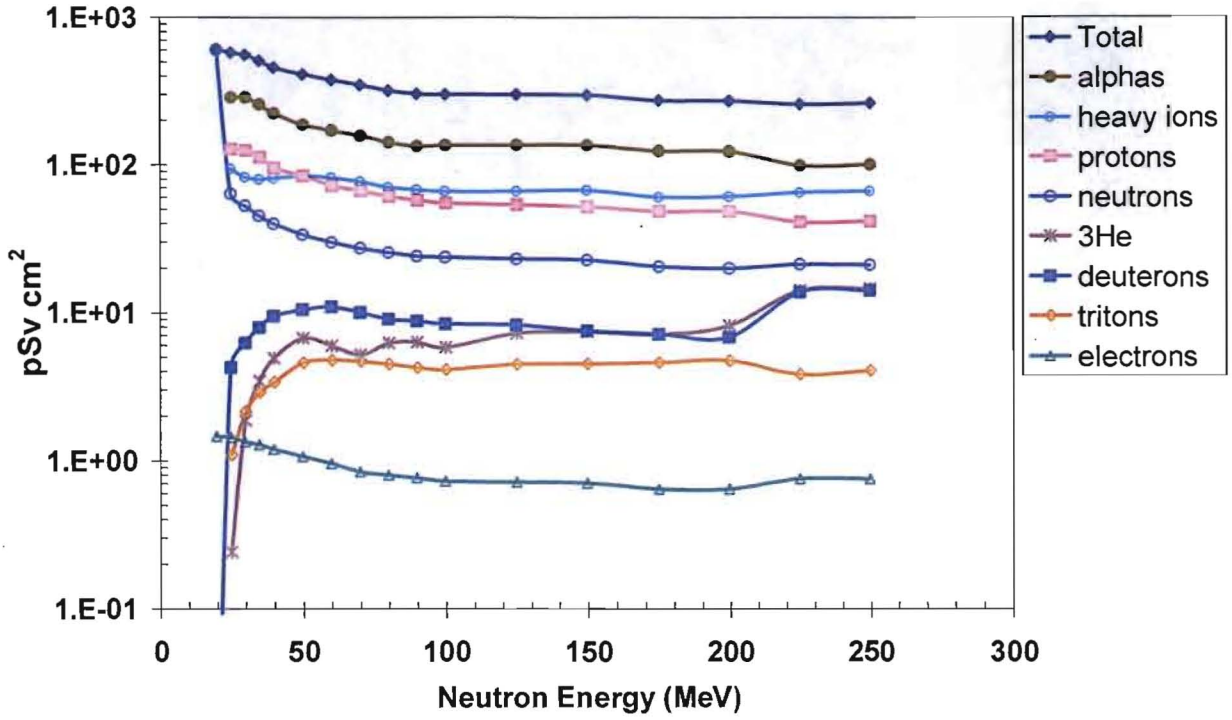
1.E+03
1.E+02
1.E+01
1.E+00
1.E-01
pSv cm2
0
50
100
150
200
250
300
Neutron Energy (MeV)
Total
alphas
heavy ions
protons
neutrons
3He
deuterons
tritons
electrons

Figure 3

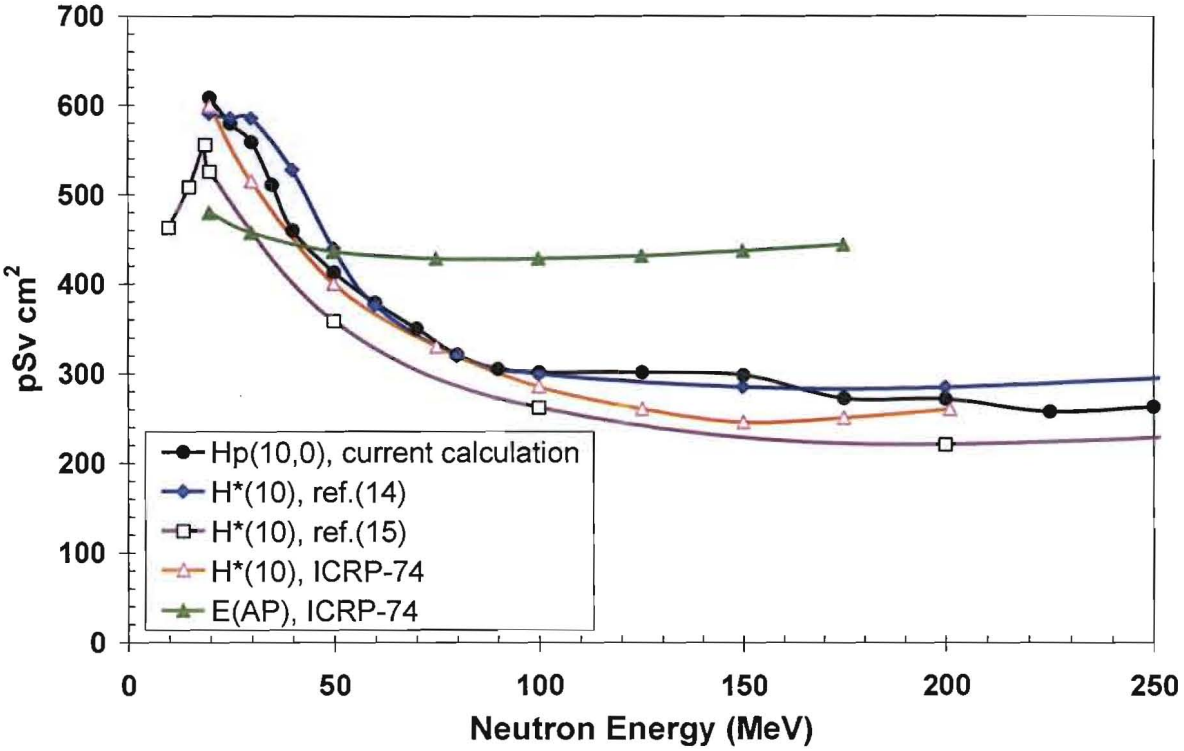
700
600
500
400
300
200
100
0
pSv cm^2
0
50
100
150
200
250
Neutron Energy (MeV)
Hp(10,0), current calculation
H*(10), ref.(14)
H*(10), ref.(15)
H*(10), ICRP-74
E(AP), ICRP-74